Comprehensive Comparison of Different Models for Large-Scale Thermal Energy Storage

Fabian Ochs[1,*] Abdulrahman Dahash[1], Alice Tosatto[1], Michael Reisenbichler[2], Keith O'Donovan[2], Geoffroy Gauthier[3], Christian Kok Skov[3], Thomas Schmidt[4]

[1] *Unit of Energy Efficient Buildings, University of Innsbruck, Innsbruck, Austria*
[2] *AEE - Institute for Sustainable Technologies, Gleisdorf, Austria*
[3] *PlanEnergi, Copenhagen, Denmark*
[4] *SOLITES - Steinbeis Research Institute for Solar and Sustainable Thermal Energy Systems Stuttgart, Germany*
[*] *Email: Fabian.Ochs@uibk.ac.at*

ABSTRACT—Large-scale thermal energy storages (TES) are advantageous to bridge the seasonal gap between heat demand and availability of renewables. However, the high investment costs associated with large-scale TES is still seen as a major barrier. Among others, challenges are space availability and the presence of groundwater. The complexity of the processes and interactions motivate the application of simulation tools for planning such systems. For TES optimization, flexible and detailed models are required that allow to investigate different geometries, insulation levels and boundary conditions, e.g. presence of groundwater (GW). In contrast, fast and easy-to-use models are required for simulations of a TES integrated in a larger system. In this work, different TES models are compared in various simulation platforms: COMSOL Multiphysics, TRNSYS, Modelica/Dymola and MATLAB/Simulink.

The paper summarizes the features of the different TES models, shows the different concepts to reduce the model complexity and compares the results with respect to thermal losses and temperature stratification. TES Types and geometries include buried tanks (cylinder, cuboid), pits (truncated cone, pyramid stump) and hybrids (cylinder with cone stump, cuboid with pyramid stump). TES can be built either completely buried or partially buried building a dam with (part of) the excavated soil. Detailed 2D and 3D FE models developed in COMSOL Multiphysics were validated against measured data from a pit TES and were used as reference for this study. Some of the models take advantage of symmetry and cylindrical coordinates in order to reduce the model to 2D (cylinder, cone). Within this work, deficiencies could be identified, models could be improved and also the influence of the user was seen. Overall, good to acceptable agreement between the tools was achieved after a review phase and after eliminating bugs and user influence.

Keywords: Large-scale thermal energy storage; Renewable district heating; Modelling and simulation; Verification and validation, TES comparison.

1. INTRODUCTION

One of the key measures to mitigate CO_2 emissions and climate change is the systematic transition from fossil fuels to renewable energy (RE) sources. Also, the development of more reliable and efficient energy systems is a milestone to expand the share of renewables in the energy sector. Thus, large-scale seasonal thermal energy storage (STES) substantially facilitates a full exploitation of the local renewable energy sources (e.g. geothermal, solar, waste heat) potential. Thereby, it bridges the gap between buildings' heating demand in winter and the availability of varying RE resulting in an enhancement of flexibility in heat supply and demand [1].

Large-scale seasonal thermal energy storage (TES) systems are key elements for renewables-based district heating (R-DH) systems due to their capability to introduce and/or expand the share of renewables in those systems. However, Dahash et al. [2] demonstrated the complexity and a number of factors that play a role in limiting those systems from being expanded to practical applications. Crucial factors can be categorized under TES surroundings (e.g. ground thermal properties, groundwater flow) and TES dimensioning and design (e.g. TES volume, geometry, insulation thickness) and others [3]. Down to the fact that the focus is hot-water tanks and pits, those systems are frequently associated with high construction costs given their large scale. As a result, planners and engineers must ensure that a TES is suitably planned

prior to construction in order to not violate constraints of economic feasibility and efficient operation [2]. Subsequently, numerical simulations allow for an in-depth understanding of TES operations, thus enabling the planners to optimize the design and develop the operation [4].

Within the framework of a design phase, several components of the TES (e.g. water domain, cover and insulation) must be considered as a whole in order to establish a detailed study on the TES. Such an investigation is often seen as "component level modelling", where the TES is thoroughly analysed [5], whereas the integration of TES into the overall energy system (e.g. district heating) is classified as "system level modelling" [6]. Hence, the first level (TES design level) plays a critical role in the definition of the effective performance of the TES, whereas the second level pays significant attention to the integration and operation of TES within a larger system. In this context, it must be pointed out that thermal losses are inevitable when considering the high temperatures involved in the TES operation and, accordingly, this might significantly affect the DH system capacity leading to challenges in meeting the load requirements effectively. The behaviour of the TES envelope quality (materials) is dependent on several aspects (e.g. temperature, humidity, leakages from the TES, material degradation, fatigue) [7]. Consequently, these aspects must also be considered at the component level since they represent a critical cost item [8]. Accordingly, the TES lid can also be modelled in detail and categorized under component level modelling.

As TES is hosted by the subsurface for a minimum lifetime of 30 years (or better 50 years), it is crucial to examine the influence of TES operation on the ground surroundings. In particular, some subsurface locations exhibit groundwater tables and their existence might result in some risks (e.g. increase of groundwater temperature, enhancement of contaminant transport, poor groundwater quality). Therefore, several national authorities issue regulations that set predefined values to maintain high groundwater quality. Out of these regulations, some European countries (i.e. Germany and Austria) restrict the groundwater temperature to a maximum of 25°C. Thus, a third level arises, which is known as the hydrogeological level in which the TES interaction with the ground is examined [9].

Bearing the aforementioned challenges of a fully buried TES system in mind, a proper planning layout is essential to ensure the economic feasibility of the project and, then, commissioning the TES. Thus, the authors report the development of several numerical TES models that are established in a number of modelling environments and tools. Such tools are COMSOL Multiphysics, MATLAB/Simulink, Modelica/Dymola and TRNSYS. These tools are capable of capturing the different design and modelling levels (i.e. system, TES, hydrogeological level) involved in the TES planning. Next, the work compares the outcomes of the different TES models under a set of given boundary conditions. The energy balance of the TES models, the TES stratification profile and the ground temperatures are compared in order to ensure a successful calibration.

2. STATE-OF-THE-ART IN NUMERICAL MODELLING AND SIMULATION OF LARGE-SCALE TES

Thermal energy storage emerges as an effective player in the energy transition to renewables-based heat supply. Thanks to TES's capability to store heat and make it available on-demand, it concretely assists in the establishment of R-DH systems, whereby large shares of renewables are anticipated for integration.

Figure 1 reveals the TES modelling process hierarchy, whereby at the early phase of TES construction, a pre-design tool is often used for the planning phase and, then, details are consecutively included into the model until it reaches a detailed model. Next, the TES undergoes a technology investigation as it is integrated within an energy system (e.g. R-DH system). Accordingly, the TES technology is thoroughly evaluated and the outputs are post-processed producing some optimization proposals (e.g. optimal construction type, optimum TES geometry and optimal insulation thickness). Meanwhile, Dahash et al. [6] pinpointed that there exist three factors, which strongly influence the computation time: level of detail (pre-design, detailed), number of components (technology integration) and simulation time step (e.g., hourly, daily). These players might substantially affect the computation time as shown in Figure 2. In order to optimally select the right level, the aim of the analysis should be defined beforehand [4].

Given the complexity seen when modelling DH systems and the thermo-hydraulic behaviour of large-scale TES (stratification, buoyancy, etc.), a wide range of tools is commonly employed in modelling DH and TES systems. Such tools are commonly categorized into five types:

- Energy system simulation (ESS) that involves tools like Modelica/Dymola, TRNSYS, MATLAB/Simulink;
- Building physics envelope heat and mass transfer tools such as WUFI Pro and Delphin;
- Computational fluid dynamics (CFD) such as ANSYS Fluent and CFX;
- Multiphysics tools such as COMSOL Multiphysics (which is also used for building envelope heat and mass transfer); and
- Subsurface simulation tools such as FEFLOW (flow, mass and heat transport processes).

Consequently, it is crucial to highlight that different discretization schemes are employed in simulation tools. Herein, the spatial discretization of the domain is executed using either finite element method (FEM), finite difference method (FDM) or finite volume method (FVM). Besides, the level of detail depends on the model's dimensionality. For instance, highly-detailed models require 3-D representation and as the level of detail becomes less important, then the model can be reduced to 2-D or 1-D models. The importance of 3-D models arises due to complex TES geometries and presence of groundwater.

ESS tools (e.g. Modelica/Dymola, TRNSYS) often employ FDM as discretization fashion for models represented as 0-D or 1-D. Yet, it is possible to develop 2-D models in such tools but the computation time might exceed the limits. On the other hand, CFD tools (e.g. ANSYS Fluent) require exact representation for the investigated case and, thus, 2-D or 3-D representation become more important.

Figure 3 shows the allocation of the aforementioned tools to the different levels where they can fit the best. There, it is seen that those tools are the widely used ones to cover the different aspects of buried TES and its surroundings. At the DH level, TES models discretized in FDM are the most broadly used ones, as this level primarily aims to examine the TES interaction with the DH system FEM models, however, are in need for the TES level as this level targets the detailed TES design. Furthermore, specific tools (e.g. FEFLOW) are required if the hydrogeological aspects due to TES construction must be inspected.

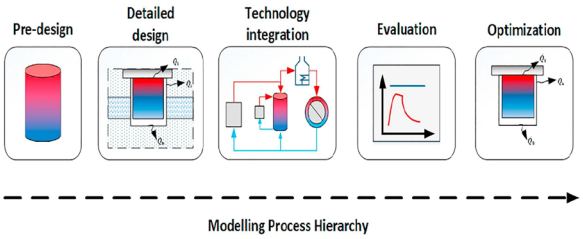

Figure 1 An exemplary hierarchy for modelling process of large-scale TES in DH systems (reproduced from [6]).

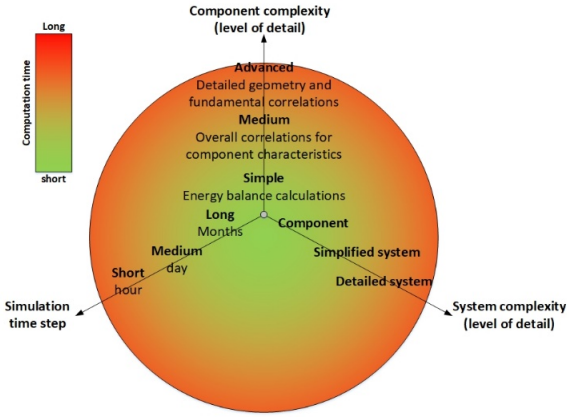

Figure 2 Computation time for TES simulations depending on the level of detail (reproduced from [6]).

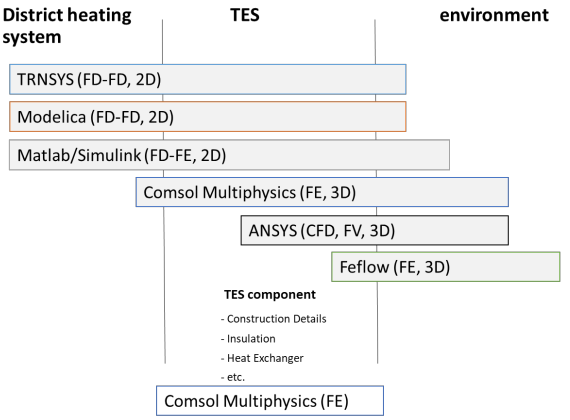

Figure 3 Representation of simulation levels with allocation of several tools used according to their scope (discretization scheme of fluid domain and solid domain: FDM finite difference method, FEM finite element method, FVM finite volume method, CFD computational fluid dynamics).

2.1 TES Model Features

Starting the review with TRNSYS [10], there exists several commercial so-called coarse-structure models. The XST model (type 342) simulates buried cylindrical water tanks [11]. The other is the ICEPIT-model (type 343), which can represent buried gravel-water pits, for instance. The ICEPIT-model simulates truncated cones, whilst the XST-model simulates only cylindrical tanks [2]. Moreover, the engineering consulting company (TESS) developed a 3D model for TES simulations in TRNSYS based on special

requests. The 3D model (type 1322) has two symmetry planes, which means that it represents only a quarter of the TES. The model is capable to capture the pyramid stump geometry and it has a built-in coupling to the surrounding soil. In case it is needed to model a truncated cone, then it is possible to coupe two other components one to represent the cone TES (type 1300) and the other stands for the soil (type 1301). The TES type 1300 has same features as type 1322 except the geometry modelled.

A finite difference fluid domain coupled to a finite element solid domain model implemented in Matlab/Simulink using s-functions was presented by Ochs [12, 13], which can model cylindrical and conical underground TES.

In Modelica/Dymola, there exists a number of TES components in several Modelica-based libraries. Among others, the Modelica Buildings library [14] is one of the leading libraries in the field of building and district energy systems whereby different TES components can be found. In this regard, Köfinger et al. [15] performed a simulation-driven evaluation for the utilization of waste heat in Linz DH system. Then, the authors paid attention to the integration and operation of seasonal TES in the considered system. To emulate the system and TES, the components were used from the Modelica Buildings library. Yet, the calibration of the TES model for large-scale was not demonstrated despite the usability and validation of the TES models for small scale (1 m^3 – 10 m^3). In this context, Dahash et al. [7] developed the TES model "stratified" in this library and extended its capabilities to represent large-scale TES systems. Later, the work cross-compared the developed model against a FEM model, which was validated against measured data from Dronninglund pit TES [4]. However, this Modelica TES model is still under development to represent different TES geometries (e.g. truncated cone) as part of the Modelica-based library (UIBK_DisTES) that aims to develop thermo-hydraulic models for district energy systems at the University of Innsbruck. Another large-scale TES model in Modelica based on the Buildings library was developed by Reisenbichler et al. [16] and was compared against measured data from the pit TES in Dronninglund.

In a different tool, a dynamic model for a solar DH system with a seasonal TES was presented in [17]. The dynamic model was developed in Aspen HYSYS software to represent the solar-assisted DH system in Vojens, Denmark. Since this tool offers only cylindrical tanks, the PTES installation was approximated to a tank with same upper circumference and volume. Furthermore, the tank model is a fully-mixed component and, thus, different tank elements had to be connected in series to develop a stratified tank. The proposed modelling approach led to results that significantly differed from the actual installation.

In an attempt to condense the computational efforts, van der Heijde [18] utilized time aggregation algorithms (i.e. representative days) to represent an S-DH system equipped with a seasonal TES. It was revealed that the algorithm is computationally cheaper by 10-30 times when compared to simulations without aggregation. Yet, it was concluded that the minimum required number of representative days was not obtained. On a brighter note, the algorithm was recently used to determine the optimal design and control of a fictional district energy system of the city of Genk, Belgium [19].

Furthermore, Sorknæs [20] developed a simulation method that is capable enough to capture the dynamics of PTES coupled with a heat pump in an S-DH system. The method was tested by comparing the simulated results against the measured data from Dronninglund pit TES for the year 2015. Accordingly, the simulated thermal losses were around 1741 MWh, whereas the measured thermal losses were 1275 MWh. This discrepancy (approx. 35 %) highlights the inaccuracy of this method, which might later lead to wrong conclusions during the STES planning phase.

All the aforementioned models were limited by many factors. For instance, the model can be restricted to one geometry (i.e. tank) and is incapable of representing sloped-wall TES geometries, or the developed models rely on a simple representation for the surrounding ground leading to a major shortcoming if the surrounding contains groundwater flow. As a result, Dahash et al. [4] recently developed a FEM model that represents large-scale TES in COMSOL Multiphysics. The developed model took advantage of the axisymmetric feature in COMSOL Multiphysics and thereby it allows to model a single-half of the TES with circular cross-section. As a result, the number of equations can be reduced with a 2D axisymmetric model.

2.2 Contribution of this work

Given the different levels associated with TES planning, this work investigates the differences between the different tools considering TES level modelling. In other words, the work focuses on the comparison between the TES models in a number of tools in order to highlight the applicability of each tool and its capability. To do so, it is important to consider

different TES geometries and boundary conditions. This work will focus on cylindrical tanks with different insulation levels. Other geometries such as cone and pyramid will be considered in future work.

3. Methodology

3.1 TES Models

In principle, the different TES models are developed relying on a similar concept, i.e. coupling a fluid domain model (typically 1D-FD) to a solid domain model (typically 2D, FD or FE). The common feature among the different models is that they all take advantage of the axisymmetric representation for tank geometries. Yet, this feature is extended in some tools (i.e. COMSOL Multiphysics, MATLAB/Simulink and TRNSYS) to further simulate the truncated cone, whereas the efforts are still ongoing to implement this feature in Modelica/Dymola.

Figure 4 schematically shows the TES system in interaction with the surrounding ground. Therein, it is seen that the TES is equipped with so-called multiport for charging/discharging processes. Thus, the TES fluid domain is developed as a multiport model allowing the height of the ports to be specified and TES can be discretized into a number (n) of segments that are considered with equal volumes rather than equal distances (i.e. equidistant heights). For each segment (i), conductive and convective heat transfer mechanisms are considered in an energy balance

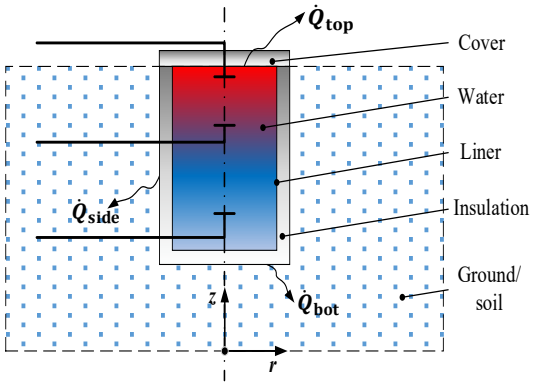

Figure 4 An exemplary 2-D representation of an underground tank with the different required domains and surroundings [21].

expressed as a partial differential equation as follows:

$$\left(\rho A_i c_p\right)\frac{\partial T_i(t)}{\partial t} = -\left(\rho \dot{V}_w c_p\right)\frac{\partial T_i(t)}{\partial z_i} \quad (1)$$

$$+A_i \frac{\partial}{\partial z_i}\cdot\left(\lambda_w \frac{\partial T_i}{\partial z}\right) - \dot{q}_{loss,i}$$

$$\dot{q}_{loss,i} = U_{side} \cdot P_i \cdot \left(T_i(t) - T_{g,i}(t)\right) \quad (2)$$

where ρ, c_p and λ_w represent the density, specific heat capacity and thermal conductivity of the storage medium, respectively. Whereas A_i is the cross-section area of the segment (i). Equation (2) expresses the thermal losses from the corresponding segment (i) to the surroundings and, therein, U_{side} stands for the overall heat transfer coefficient (HTC) of the TES envelope (fluid to ground). Whilst (P_i) is the segment perimeter.

Moreover, the heat transfer also occurs in the ground and it is described by the following equation:

$$\left(\rho_g c_{p,g}\right)\frac{\partial T_g(t)}{\partial t} = \nabla \cdot \dot{q} \quad (3)$$

COMSOL Multiphysics permits a spatial discretization in a finite-element fashion, whereas Modelica/Dymola and TRNSYS allow a spatial discretization following the finite-difference method. Having the advantages of both discretization methods, the TES fluid domain in MATLAB/Simulink is developed as an FD model that is coupled with an FE ground model, see Table 1.

In addition to the discretisation scheme, also the mesh refinement differs among the tools. COMSOL Multiphysics offers the highest flexibility and applies a very fine mesh (for both, solid and fluid domain), while in TRNSYS, the mesh of the solid domain is predefined and very coarse for the XST model in TRNSYS. Whereas MATLAB/Simulink uses 30 nodes for the fluid domain and a user defined refinement of the FE solid domain mesh. All FD models (TRNSYS, Modelica/Dymola) apply a logarithmic discretisation scheme, i.e. the mesh is finer close to the TES and is coarser towards with increasing radius and depth, respectively.

Besides, COMSOL Multiphysics tool allows the consideration of all multi-physical phenomena (e.g. heat transfer, fluid flow, mass transfer).

Table 1 Summary of discretisation scheme.

Model	Fluid Domain	Solid Domain	Geometry
COMSOL	1D FE	2D/3D FE	Various
TRNSYS	1D FD	2D FD	Cylinder/Cone
MODELICA	1D FD	2D FD	Cylinder
MATLAB	1D FD	2D FE	Cylinder/Cone

3.2 Stratification and Buoyancy

Large-scale seasonal TES systems often experience lengthy storage periods in order to fulfil the seasonal tasks. In absence of forced convection or enthalpy flowrates during such standby phases, a buoyancy-driven natural convection heat flow dominates. This phenomenon arises since water has a temperature-dependent density. Hence, a natural convection process is accordingly induced by buoyancy. As a result, a recirculation of water occurs between the hot and cold regions close to the TES boundaries. Given the fact that a high degree of losses through the top of the TES is anticipated, a drop in temperature might be observed at the very top of the storage near to the upper surface area. This drop might result in an undesired phenomenon known as "inverse thermocline" or "thermocline inversion" in the simulated stratification profile.

In order to tackle the aforementioned shortcoming, the water heat conductive term in Equation (1) is substituted with another term to enhance the thermal conductivity of water and, subsequently, allow buoyancy driven mixing and thus eliminate the occurrence of inverse thermocline [4]. The different tools, which are compared in this work, implement different functions to tackle this undesired behaviour and allow the TES water to mix. In TRNSYS-XST, the layers with inversed thermocline are simply mixed. For instance, UIBK COMSOL Multiphysics and UIBK Modelica numerical models are based on power law correlations and allow for a rapid or slow mixing rate considering a parameter that can be tuned up or down. Besides, the implementation of this function comprises the segmental temperature difference $\partial T_i / \partial z_i$ in both tools. Also in MATLAB/Simulink and AEE INTEC's Modelica model, buoyancy models are based on power law correlations, i.e.

$$\lambda_{\text{mix}} = C \cdot |\Delta T|^n \cdot (\Delta T < 0) \quad (4)$$

where n typically takes values between 0.4 and 0.5 and C is a tuning parameter.

3.3 Operation Scenario and Boundary Conditions

As this work aims to develop and cross-compare numerical models that are suitable for the different levels of the modelling process, system simulations are eliminated at this stage in order to simplify the modelling scheme and, consequently, no DH system is simulated. The DH operation, however, plays a significant role in the charging/discharging phases of the TES component. Thus, an excel-based tool known as the "Load Profile Generator" is utilized to simulate a district with 833 highly-efficient buildings each with a nominal heating load of approx. 2 kW. Next, it incorporates a heat source with a constant power (e.g. geothermal) of 1.5 MW as shown in Figure 5. The tool includes an ideal (i.e. adiabatic) three node TES component.

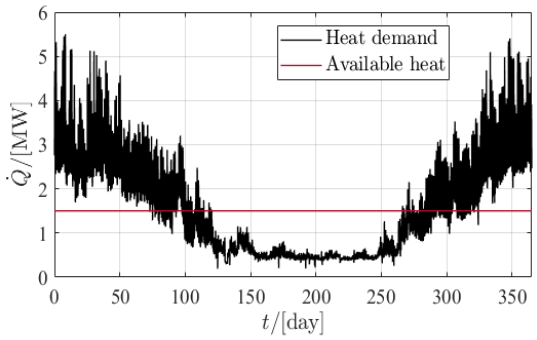

Figure 5 Available heat source and heat demand of the considered district as simulated in the "Load Profile Generator" tool (giga_TES) with hourly-resolution.

The flowrate for charging/discharging was defined starting from the load curve and the heat source curve. Throughout the charging phase, the available energy from the heat source is used to satisfy the summer load and the remaining excess portion is stored in the TES. In contrast, the available energy from the heat source is used to satisfy part of the winter load, then the required remaining power is extracted from the TES over the discharging phase. Accordingly:

$$\dot{V}_{\text{ch/dis}} = \frac{\dot{Q}_{\text{source}}(t) - \dot{Q}_{\text{load}}(t)}{\rho \cdot c_p \cdot \Delta T} \quad (5)$$

Thus, time-series inputs are used for the temperature and flowrate at both inlet/outlet ports of the examined TES component. Figure 6 and Figure 7 show the flowrate and the corresponding temperature time-series used for the TES operation. There, the positive flowrate stands for the charging process and the negative represents the discharging. The work assumes a constant DH supply temperature of 90 °C and a return temperature of 60 °C. For the comparison of the models, an underground (buried) tank with a volume of 100,000 m^3 and a height of 25 m is used, see Figure 8.

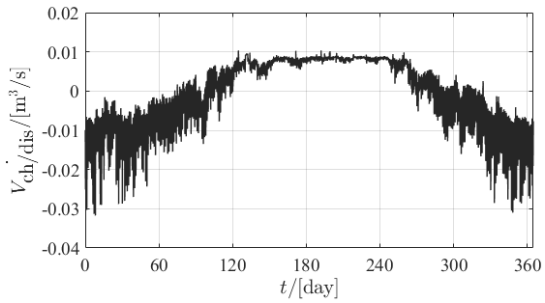

Figure 6 Charging (+)/discharging (-) flowrate as annual periodic function for a 100,000 m³ TES.

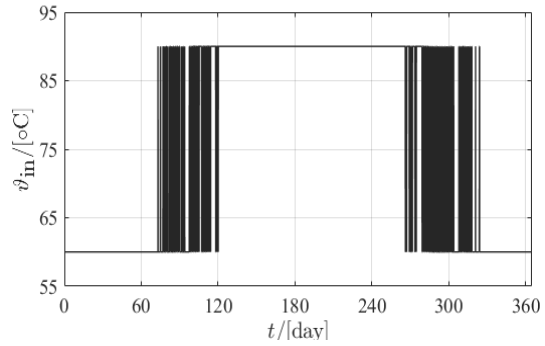

Figure 7 Flow temperature as a periodic function of the time.

The tank is initialized with a temperature of 10°C, which is equivalent to the ground initial temperature. The ambient temperature is expressed as below:

$$T_{amb} = 283.15 - 10 \cdot \cos\left(\frac{2\pi \cdot t}{365 \cdot 24 \cdot 3600}\right) \quad (6)$$

The TES is surrounded by ground (soil) with a density of 2000 kg/m³, specific heat capacity of 880 J/(kg·K) and thermal conductivity of 1.5 W/(m·K). Figure 8 shows the ground domain with its relevant dimensions.

In order to comprehensively verify the numerical TES models and understand their operational impact, it is also crucial to compare the soil temperatures at selected locations in the TES surroundings. The soil temperature shall include not only the neighbouring soil of TES lateral environment, but also the soil beneath the TES. This is attributed to the fact that in several countries (e.g. Germany, Austria) there are national standards prescribing that the soil temperature should not exceed a certain value. Therefore, this work compares the soil temperatures at two lines in the TES surroundings.

In this context, Figure 9 displays a vertical line with a distance of 1 m next to the TES sidewalls. Along that line, the soil temperature is extracted at 5 locations with a relative height of (h^* = 0, 0.25, 0.5, 0.75 and 1) as they are highlighted by green-filled circles. It must be pointed out that the temperature at (h^* = 1) is strongly affected by the ambient temperature as it is exposed to the ambient air. Furthermore, Figure 9 shows a horizontal line with 3 green-filled circles. At those locations, the soil temperature beneath the TES should also be compared in order to fully verify the TES and its surroundings models. These locations are: r = 0, r_{TES}/2 and r_{TES}. Moreover, another comparison point is chosen as shown by the red-filled circle. Having this point considered, the comparison locations form a similar geometry to the TES considered with a height of (h_{TES} + 1 m) and a radius of (r_{TES} + 1 m).

Given the fact that the TES insulation level (on the top, sidewalls and bottom) plays an essential role in the techno-economic performance of the TES and the groundwater protection, it becomes crucial to examine

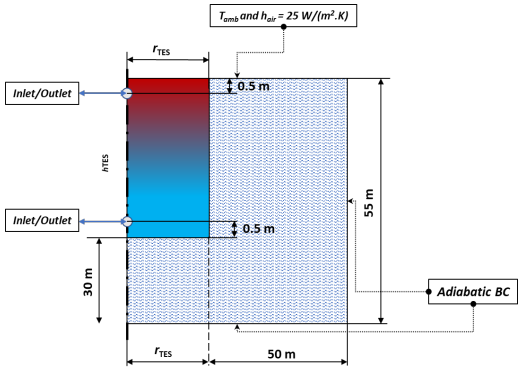

Figure 8 Simplified TES scheme used for model comparison.

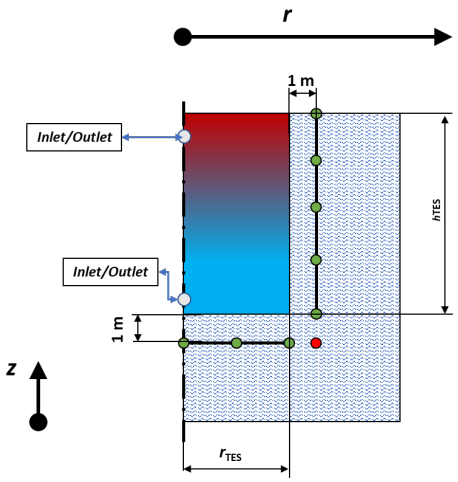

Figure 9 Location of evaluated ground temperatures.

the TES under several insulation cases. Accordingly, the comparison cases are categorized into two primary items: “non-insulated” and “insulated”. Each major item is subdivided into three minor cases considering different values for the insulation of the lid (TES cover). A total number of 6 cases (see Table 2) are considered for each model in the comparison. In this regard, the non-insulated cases are labelled with (Case 1), whereas the insulated cases are assigned to (Case 2). To distinguish between the different levels of lid insulation, the alphabets (a, b and c) are used to indicate the values of U_{top} = 0.05 W/(m^2·K), 0.1 W/(m^2·K) and 0.15 W/(m^2·K), respectively.

3.4 Simulation Setup and Preconditioning

Throughout the initial phase of TES operation (3 to 5 years), the large-scale buried TES has lower efficiency depending on the insulation level and quality. Yet, it cannot be avoided. This is attributed to the fact that this phase preheats the ground until it reaches a thermal equilibrium. Therefore, the cases 1 (non-insulated) should run for 10 years, whilst cases 2 (insulated) run for 5 years. Each simulation year has 365 days (no leap year, 8760 hours). The evaluation is based on the last year of results.

The TES starts the operational year with a discharging phase and due to the fact that the TES is initialized with a temperature of 10 °C, it would not be capable of providing any useful energy to the R-DH network. Thus, the simulations start on April 20th (beginning of charging phase, see Figure 6) and carry on until the end of the examined case (5 or 10 years). Accordingly, the simulation start time is set to 9,417,600 [sec] as it represents the 20th of April of the first simulation year.

Herein, case 1 simulations ran for 10 years in order to allow the TES to pass the preheating phase and the TES operation gets into quasi steady state. Whereas case 2 simulations were carried out for 5 years.

Both Figure 10 (a) and (b) reveal the breakdown of thermal losses for the last year of each examined case. Besides, both figures report the total thermal losses and the contributions from cover (top), side wall and bottom.

Figure 10 depicts overall relatively good agreement between the tools, but also a discrepancy in the total thermal losses for the non-insulated cases at the end of the (10th) year. Therein, it is clearly seen that the top contribution of the thermal losses is comparable between all tools. The major discrepancy is attributed to the sidewall contribution, whereas a slight discrepancy is seen for the bottom. Besides, it is worthwhile to mention that the total deviation between COMSOL Multiphysics and Modelica is only approx. 2 %. The main deviations of TRNSYS can be explained by a combination of a thermal bridge at the cover-side wall intersection and the relatively coarse mesh. Another slight difference can be explained with different assumptions for the cover insulation. The models implemented in MATLAB/Simulink, Modelica/Dymola and TRNSYS assume the fluid domain starts at ground surface level and considers the cover as a resistance, while in COMSOL it is 1 m below the ground with a physical layer for the cover insulation. The thermal bridge is avoided in MATLAB and Modelica by implementing an overlap. Yet, this is not possible in the XST model of TRNSYS.

4. RESULTS AND DISCUSSION

4.1 TES operation – Energy balance

Table 2 Summary of the cases considered in the cross-comparison; 1: non-insulated at side walls and bottom, 2: insulated at side walls and bottom.

Case	Subcase	U_{top} [W/(m^2·K)]	U_{side} [W/(m^2·K)]	U_{bot} [W/(m^2·K)]
1	a	0.05	90	90
	b	0.1	90	90
	c	0.15	90	90
2	a	0.05	0.3	0.3
	b	0.1	0.3	0.3
	c	0.15	0.3	0.3

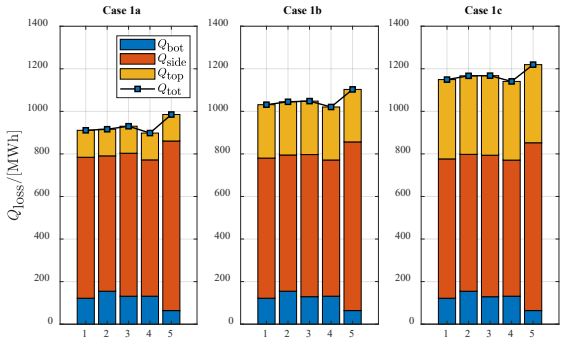

(a) non-insulated TES in 10th year of operation

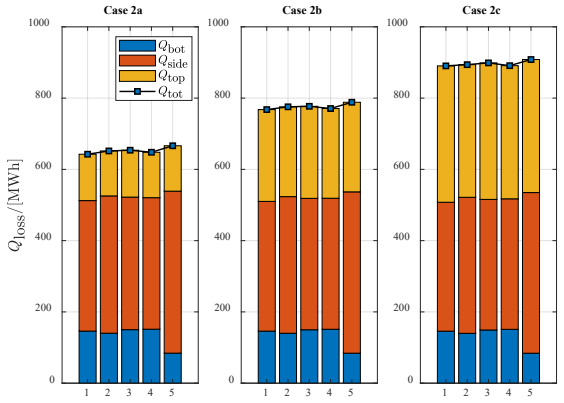

(b) insulated TES in 5th year of operation

Figure 10 Breakdown of the thermal losses for 1: UIBK COMSOL Multiphysics, 2: UIBK MATLAB/Simulink, 3: UIBK Modelica, 4: AEE INTEC Modelica and 5: PlanEnergi TRNSYS.

On a brighter note, the discrepancy among all numerical models remarkably decreases (< 2 %) for the insulated cases as displayed in Figure 10 (b). This is attributed to the fact that a smaller amount of thermal energy is transferred to the ground from the storage. In this regard, it is essential to highlight that the ground discretization and ground coupling plays a role in the calculations, particularly when large amounts of energy are transferred from the TES to the ground and, therefore, better ground discretization is required. In other words, the TES-ground coupling might be improved for the deviating numerical models in order to reduce the discrepancy when no insulation is used. Yet, it is important to point out that this leads to a significant increase in the computation time and might not be feasible in the context of system simulations.

The TES with insulation has a significantly better performance than that installed without insulation (the total annual thermal losses 650 MWh in the best case compared to 1150 MWh in the worst case). Therefore, this highlights the role of techno-economic analysis for the planning phase of large-scale TES systems.

In TES systems, the extracted thermal energy is always less than that charged or even stored, which is strongly attributed to the existence of some inevitable losses and irreversibility inherent in the standby process. Therefore, when planning a R-DH system with STES, special attention is paid to the energy discharged from STES because this has an influence on the operation of back-up heating units.

Hence, Figure 11 presents a comparison of charging/discharging energy for the different models considering the insulated cases (cases 2). Therein, the positive values stand for energy charged into TES, whereas the negative values represent the energy discharged from the TES.

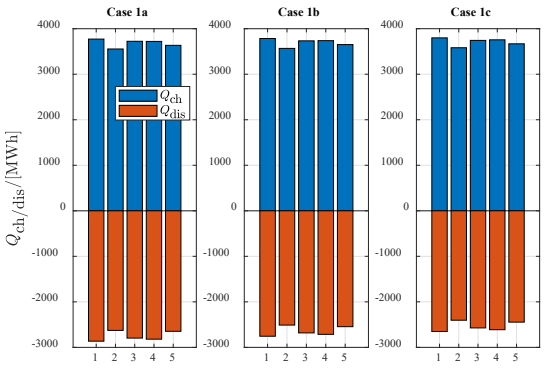

Figure 11 Comparison of charged (+)/discharged (-) energy into/from TES for the different tools under insulated TES conditions for the 5th year. 1: UIBK COMSOL Multiphysics, 2: UIBK MATLAB/Simulink, 3: UIBK Modelica, 4: AEE INTEC Modelica and 5: PlanEnergi TRNSYS.

4.2 TES operation – Temperatures and Stratification

The temperature profile at selected relative heights is compared for the different tools. The relative height is expressed as follows:

$$h^* = \frac{h_i}{h_{\mathrm{TES}}} \tag{7}$$

Figure 12 and Figure 13 exhibit the temperature profiles at selected relative heights of the TES (0.05, 0.1, 0.25, 0.5, 0.75, 0.9 and 0.95).

Therein, a relatively good matching is revealed among the examined tools in terms of TES stratification development. Besides, all models are capable of capturing the dynamic behaviour. Yet, a discrepancy between COMSOL's numerical model and the other models is noticed during periods of rapid temperature increase or decrease. The main reason for the deviation is likely the discretisation of the fluid domain (number of fluid nodes) and/or the buoyancy model or a combination of both, but further investigation is required to confirm this assumption.

4.3 TES Operation - Soil Temperature

Since the TES is hosted in the subsurface, it is also important to compare the soil temperature in the TES surroundings e.g. in order to find out whether the predefined legal regulations are violated in terms of temperature exceeding. Prior to the comparison, it is important to underline that the soil domain is discretized using FEM in COMSOL Multiphysics and MATLAB/Simulink, whereas FDM discretization was used for the soil in the following tools: Modelica/Dymola and TRNSYS.

The soil temperature comparison presented in Figure 14 considers two sets of temperatures: one is located vertically with 1 m distance from the TES and the other is located horizontally 1 m below the TES (see Figure 9).

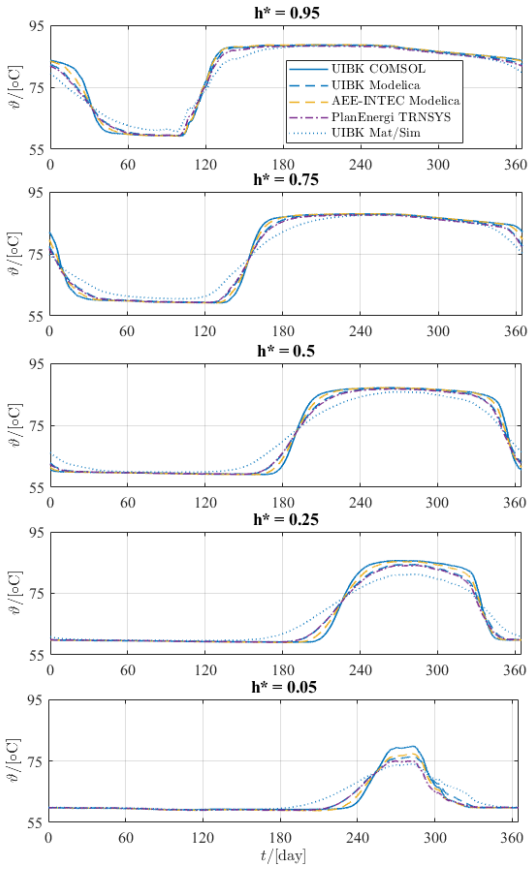

Figure 12 Comparison of temperature profiles for a cylindrical tank at selected relative heights (h^*) of the TES for non-insulated case 1b during the 10th year.

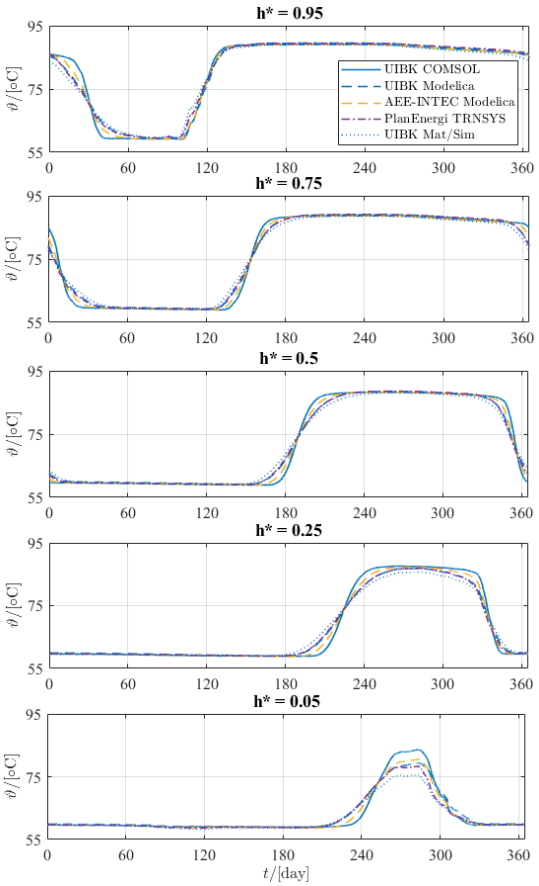

Figure 13 Comparison of temperature profile for a cylindrical tank at selected relative heights (h^*) of the TES for insulated case 2b at the 5th year.

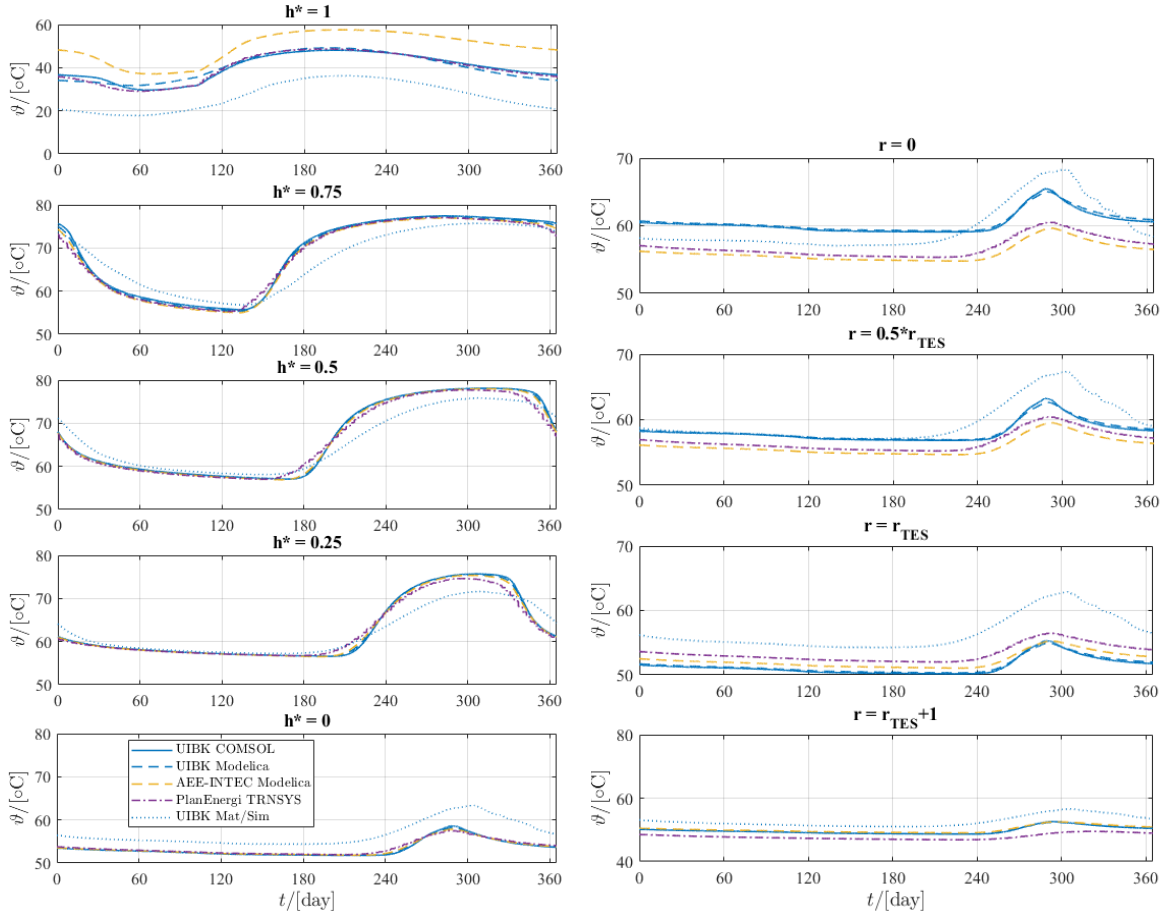

Figure 14 Comparison of the soil temperatures at selected relative heights and 1 m next to the tank TES lateral wall as well as beneath the tank TES for the non-insulated case 1b at the 10th year.

Accordingly, Figure 14a reveals the soil temperature evolution in the different tools for the non-insulated case 1b (U_{top} = 0.1 [W/(m^2.K)], U_{side} = U_{bot} = 90 [W/(m^2.K)]) at selected relative heights which correspond to the TES relative height. Therein, it is seen that the trend for the temperature at (h^* = 1) is similar for all tools and this is due to the fact that this point is exposed to the ambient. Resulting ground temperatures show the same trend and there is good agreement between COMSOL Multiphysics and UIBK Modelica. The deviations can be explained with the differences in model set-up with respect to the cover (i.e. above ground or at ground level).

Figure 14b depicts the soil temperature for the different tools at selected points located 1 m below the tank TES. There, it is clear that the overall trend is captured by the different tools. However, a deviation is notable for some tools at different locations. In this context, at the points (r = 0 and $r_{TES}/2$) the results of two tools (UIBK COMSOL Multiphysics and UIBK Modelica) are in agreement, while the tools (AEE-INTEC Modelica and PlanEnergi TRNSYS) agree with each other presenting a slight difference to the first set of tools. At the remaining points, the results of the tool AEE-INTEC Modelica came more in accordance with the results of UIBK COMSOL Multiphysics and UIBK Modelica.

For insulated case 2b, Figure 15 show the evolution of the soil temperature at 1 m next to the tank TES lateral wall and 1 m below the tank TES, respectively. There, it is notable that the trend remains similar to what case 1b revealed. However, the maximum soil temperature achieved is lower compared to that of the non-insulated case (1b) and, therefore, the deviation in the results is slightly lower.

It deems that the soil model requires better discretization in some tools to further reduce the minor deviation. Also, the location of the bottom diffuser has an impact on the TES temperature at the bottom.

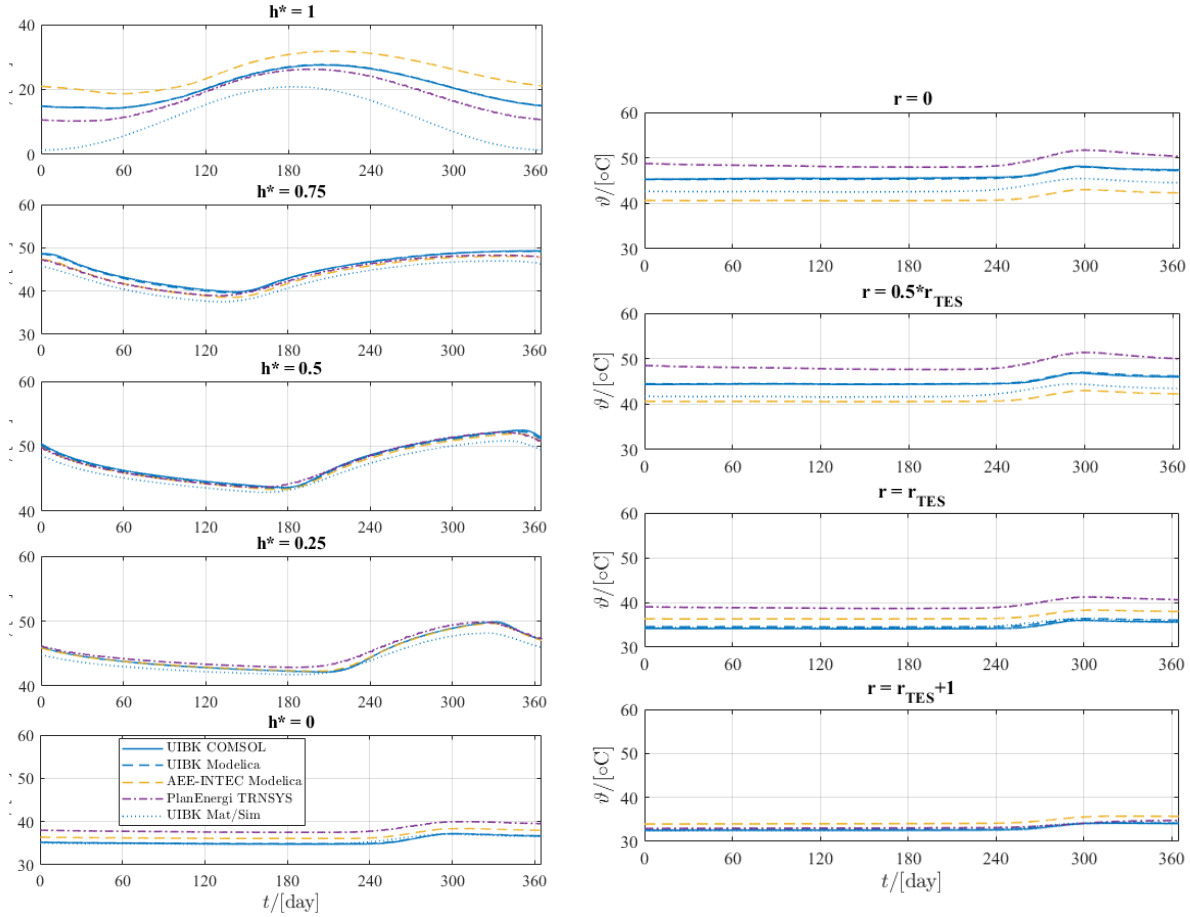

Figure 15 Comparison of the soil temperature at selected relative heights and 1 m next to the tank TES lateral wall as well as beneath the tank TES for the insulated case 2b at the 5th year.

4.4 Cooling curve – Energy Balance

Bearing in mind that Figure 6 shows the dynamic operation (i.e., charging/discharging) whereby no lengthy storage periods are seen, it becomes crucial to inspect these tools and their dynamics over lengthy storage periods. Therefore, it was decided to run a (theoretical) TES cooling operation for the different cases over 10 years in which the TES and ground initial temperatures are set to 90°C and 10°C, respectively. Such an operation will allow the user to easily spot any differences between the models for the storage phases.

Figure 16 reports the breakdown of the TES total thermal losses over the entire 10 years of cooling operation mode for two cases (case 1a and case 2a). Overall, the agreement is again, relatively good between all tools. The different tools deliver similar values for the top contribution to thermal losses. However, in particular for the non-insulated case (case 1a), there exists a notable discrepancy between TRNSYS with respect to the losses via the TES lateral wall and bottom. This led to an impact on the total thermal losses and, therefore, a deviation is noticeable. Furthermore, there exists a slight overestimation for the bottom contribution of thermal losses in UIBK MATLAB/Simulink.

It is worth mentioning that the observed trend in case 1a remains true for the insulated case (case 2a) with a major hint that the total thermal losses come closer to each other and, thus, smaller deviations are observed. This is attributed to the reduced ground coupling due to the use of insulation. This outcome confirms the conclusions drawn in the section above and the role of the thermal bridge (cover-side wall intersection) and the soil model implementation and discretization and suggests options for further improvement.

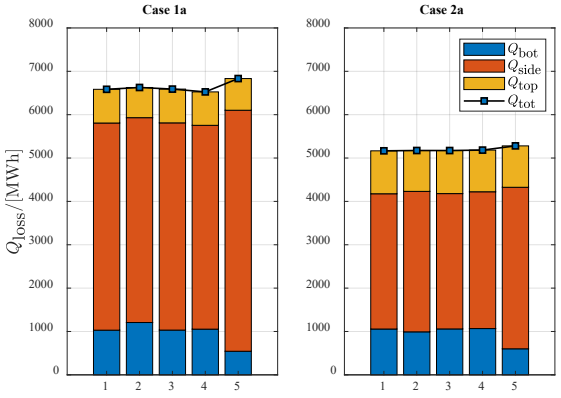

Figure 16 Breakdown of the total thermal losses for a tank TES in cooling curve operation (no incoming/outgoing flowrate) for case 1a and case 2a. 1: UIBK COMSOL Multiphysics, 2: UIBK MATLAB/Simulink, 3: UIBK Modelica, 4: AEE INTEC Modelica and 5: PlanEnergi TRNSYS.

4.5 Cooling Curve – Fluid and Soil Temperatures

Figure 17 reveals the temperature of the insulated tank (case 2a) under cooling operation conditions. There is a very good agreement for the tools notable for all the different relative heights. This agreement comes in accordance with the agreement revealed in Figure for the insulated case 2a.

Figure 18 shows the soil temperature development for the locations with 1 m next to the non-insulated TES lateral wall (case 1a) over 10 years of cooling operation. There, it is revealed that the tools are all in good agreement.

Figure 19 shows the TES temperatures decay over the 10 years of cooling operation for the non-insulated case 1a. There, notable is the agreement for all tools except TRNSYS considering the temperature at the relative heights. The temperature outcomes of

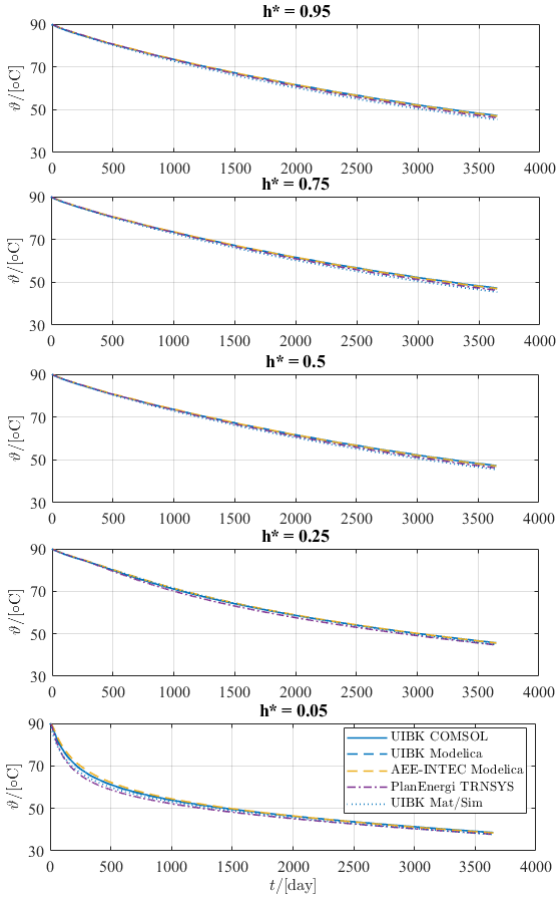

Figure 17 Comparison of temperature profile for a cylindrical tank at selected relative heights of the TES for the insulated case 2a over 10 years of cooling operation.

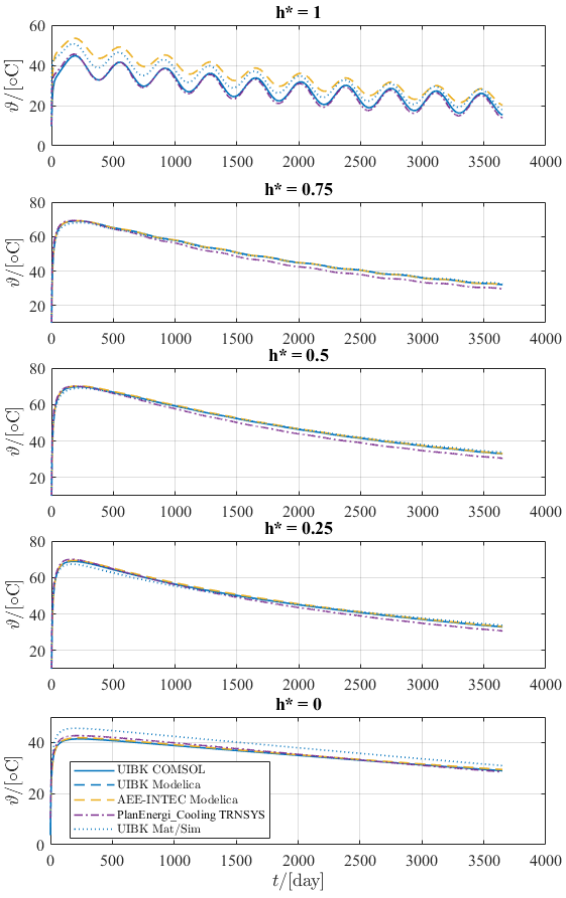

Figure 18 Comparison of the soil temperature at selected relative heights and 1 m next to the tank TES lateral wall for the non-insulated case 1a over the 10 years of cooling operation.

PlanEnergi TRNSYS are slightly lower compared to other tools which is in line with the higher losses due the above-mentioned thermal bridge. Remarkable is further the temperature of UIBK MATLAB/Simulink at the height (h^* = 0.05) as it deems this model overestimates the bottom fluid temperature. Figure 20 compares the soil temperature at selected relative heights and 1 m next to the tank TES lateral wall for the insulated case 2a over the 10 years of cooling operation in the different tools.

5. CONCLUSIONS

The planning and construction of hot-water tanks and pits is a complex interconnected process that requires a large degree of effort to ensure their economic feasibility and efficient operation. Given the large investment cost associated with such large-scale systems, the experimental real-world investigation is often seen as a challenge due to financial risks and the efficiency might drop below expectations. As a result, numerical simulations found its place favourably permitting the planners to optimize the design and develop the operation.

The work presented an approach to develop and compare numerical models for simulation of thermal energy storage (TES) systems. The presented approach is featured with reproducibility and, thus, different numerical models were implemented in several tools (i.e. COMSOL Multiphysics, Modelica/Dymola, TRNSYS and MATLAB/Simulink) by several researchers and planners involved in this work. The cooperation herein is in an international context, which demonstrated the necessity to establish solid knowledge of this field. The establishment of the different models was meant to use them in the various levels of the modelling process with an acceptable deviation between detailed-design and pre-planning models. Considering the flexibility offered with respect to the 3D modelling and the possibility to introduce the groundwater flow, COMSOL Multiphysics can be seen as a central tool for detailed

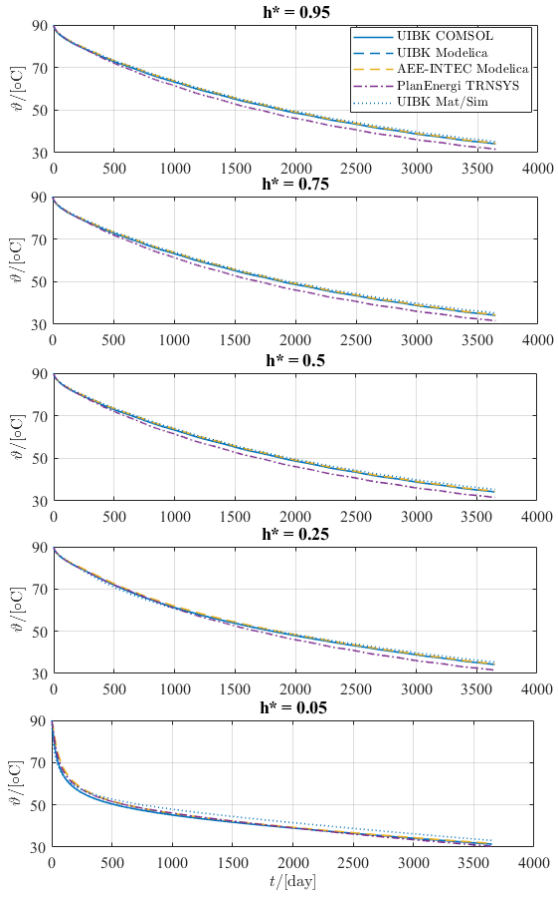

Figure 19 Comparison of temperature profile for a cylindrical tank at selected relative heights of the TES for the non-insulated case 1a over 10 years of cooling operation.

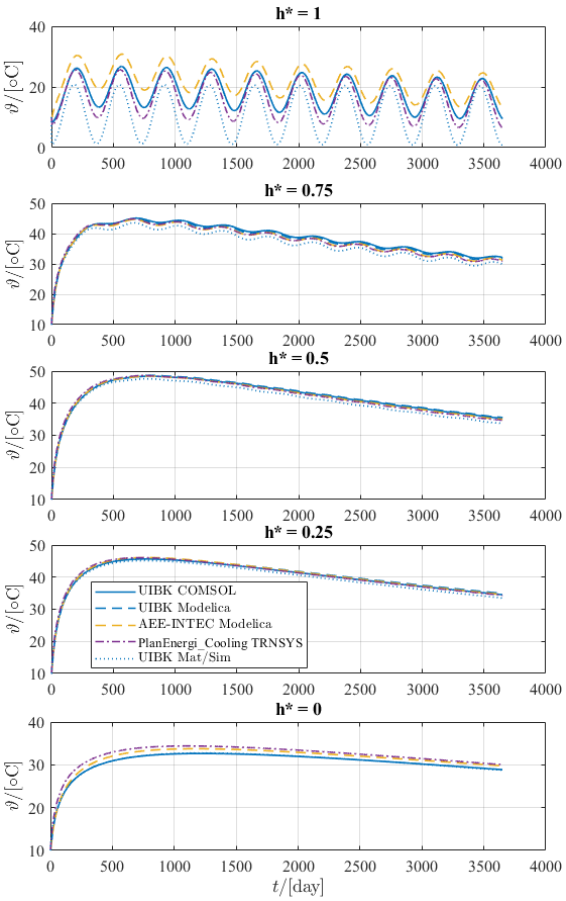

Figure 20 Comparison of the soil temperature at selected relative heights and 1 m next to the tank TES lateral wall for the insulated case 2a over the 10 years of cooling operation.

TES planning process, while TRNSYS and Modelica models have a focus on system level.

The work conducted a cross-comparison among the models considering two insulation cases. The outcomes indicated a good agreement among all models considering the energy balance contributors and temperature profiles. Yet, a deviation was observed for the non-insulated cases. In particular, the thermal bridge at the cover wall intersection and the coarse mesh in TRNSYS XST was noticed as a reason for deviations. Finer discretisation might be a solution, but further investigations are required. Furthermore, finer discretisation will cost computational performance. Lastly, another downside of the XST model is that it updates the soil temperatures only every 72 hours. This drawback cannot be changed in the standard version of the XST model.

It is important to mention that several calibration rounds were carried out until the models made it to deliver the most consistent results for the cross-comparison. Therefore, this work led to better understanding of the used models (in particular the commercial ones). Future work will include different geometries (cone, pyramid, hybrid), presence of groundwater and the comparison of the computational performance.

AUTHORS' CONTRIBUTIONS

Fabian Ochs, Abdulrahman Dahash: Numerical modelling - COMSOL Multiphysics, Modelica and MATLAB/Simulink, Writing – original draft. **Alice Tosatto**: Numerical modelling – COMSOL Multiphysics. **Michael Reisenbichler, Keith O'Donovan**: Numerical modelling – Modelica, Writing – review. **Geoffroy Gauthier, Christian Kok Skov, Thomas Schmidt**: Numerical modelling – TRNSYS, Writing – review.

ACKNOWLEDGMENTS

This project is financed by the Austrian "Klima- und Energiefonds" and performed in the frame of the program "Energieforschung". It is part of the Austrian flagship research project "Giga-Scale Thermal Energy Storage for Renewable Districts" (giga_TES, Project Nr.: 860949). Therefore, the authors wish to acknowledge the financial support for this work.

REFERENCES

[1] X. Zhou, Y. Xu, X. Zhang, D. Xu, Y. Linghu, H. Guo, Z. Wang and H. Chen, "Large scale underground seasonal thermal energy storage in China," *Journal of Energy Storage,* vol. 33, 2021.

[2] A. Dahash, F. Ochs, M. Bianchi Janetti and W. Streicher, "Advances in seasonal thermal energy storage for solar district heating applications: A critical review on large-scale hot-water tank and pit thermal energy storage systems," *Applied Energy,* vol. 239, pp. 296-315, 2019.

[3] C. Bott, I. Dressel and P. Bayer, "State-of-technology review of water-based closed seasonal thermal energy storage systems," *Renewable and Sustainable Energy Reviews,* vol. 113, 2019.

[4] A. Dahash, F. Ochs, A. Tosatto and W. Streicher, "Toward Efficient Numerical Modeling and Analysis of Large-Scale Thermal Energy Storage for Renewable District Heating Systems," *Applied Energy,* vol. 279, 2020.

[5] A. Dahash, M. Bianchi Janetti and F. Ochs, "Numerical analysis and evaluation of large-scale hot water tanks and pits in district heating systems," in *Building Simulation 2019 Conference*, Rome (Italy), 02-04 September 2019, 2019.

[6] A. Dahash, F. Ochs and A. Tosatto, "Advances in modeling and evaluation of large-scale hot water tanks and pits in renewable-based district heating," in *Proceedings of 13th International Conference on Solar Energy for Buildings and Industry (EuroSun 2020)*, 2020.

[7] A. Dahash, F. Ochs and A. Tosatto, "Simulation-based design optimization of large-scale seasonal thermal energy storage in renewable-based district heating systems," in *Proceedings of BauSIM 2020 (Virtual): 8th Conference of IBPSA Germany and Austria*, Graz, Austria, 2020.

[8] F. Ochs, A. Dahash, A. Tosatto and M. Bianchi Janetti, "Techno-economic planning and construction of cost-effective large-scale hot water thermal energy storage for Renewable District heating systems," *Renewable Energy,* vol. 150, pp. 1165-1177, 2019.

[9] A. Dahash, F. Ochs, G. Giuliani and A. Tosatto, "Understanding the Interaction between Groundwater and Large-Scale Underground

Hot-Water Tanks and Pits," *Sustainable Cities and Society,* 2021.

[10] University of Wisconsin, Solar Energy Laboratory, *TRNSYS 17: A transient system simulation program,* 2012.

[11] S. Raab, D. Mangold and H. Müller-Steinhagen, "Validation of a computer model for solar assisted district heating systems with seasonal hot water heat store," *Solar Energy,* vol. 79, no. 5, pp. 531-543, 2005.

[12] F. Ochs, "Large-Scale Thermal Energy Stores in District Heating Systems – Simulation Based Optimization," in *EuroSun 2014: International Conference on Solar Energy and Buildings*, Aix-les-Bains, France, 16 - 19 September 2014.

[13] F. Ochs, "Simulation Based Optimization of Pit and Tank Thermal Energy Storage for Solar District Heating Systems," in *3rd International Solar District Heating Conference*, Toulouse, France, 17-18 June 2015.

[14] Wetter et al., " Modelica Buildings library," *Journal of Building Performance Simulation ,* vol. 7, no. 4, pp. 253-270, 2013.

[15] M. Köfinger, R.R. Schmidt, D. Basciotti, O. Terreros, I. Baldvinsson, J. Mayrhofer, S. Moser, R. Tichler and H. Pauli, "Simulation based evaluation of large scale waste heat utilization in urban district heating networks: Optimized integration and operation of a seasonal storage," *Energy,* vol. 159, pp. 1161-1174, 2018.

[16] M. Reisenbichler, K. O'Donovan, C. R. Tugores, W. V. Helden and F. Wotawa, "Towards More Efficient Modeling and Simulation of Large-Scale Thermal Energy Storages in Future Local and District Energy Systems," *Proceedings of Building Simulation 2021: 17th Conference of IBPSA, Bruges (Belgium), 01-03 September 2021,,* 2021.

[17] K. Kubiński and L. Szabłowski, "Dynamic model of solar heating plant with seasonal thermal energy storage," *Renewable Energy,* vol. 145, pp. 2025-2033, 2019.

[18] B. van der Heijde, A. Vandermeulen, R. Salenbien and Lieve Helsen, "Representative days selection for district energy system optimisation: a solar district heating system with seasonal storage," *Applied Energy,* vol. 248, pp. 79-94, 2019.

[19] B. van der Heijde, A. Vandermeulen, R. Salenbien and L. Helsen, "Integrated Optimal Design and Control of Fourth Generation District Heating Networks with Thermal Energy Storage," *Energies,* vol. 12, no. 14, 2019.

[20] P. Sorknæs, "Simulation method for a pit seasonal thermal energy storage system with a heat pump in a district heating system," *Energy,* vol. 152, pp. 533-538, 2018.

[21] A. Dahash, M. Bianchi Janetti and F. Ochs, "Detailed Axial Symmetrical Model of Large-Scale Underground Thermal Energy Storage," in *Proceedings of the 2018 COMSOL Conference*, Lausanne (Switzerland), 22-24 October 2018, 2018.